Confined Catalysts

DOI: 10.1002/ange.200805273

An Efficient Strategy to Drive Nanoparticles into Carbon Nanotubes and the Remarkable Effect of Confinement on Their Catalytic Performance**

*Eva Castillejos, Pierre-Jean Debouttière, Lucian Roiban, Abderrahim Solhy, Victor Martinez, Yolande Kihn, Ovidiu Ersen, Karine Philippot, Bruno Chaudret, and Philippe Serp**

The possibility of using the inner cavity of a carbon nanotube (CNT) as a nanoreactor of a few nanometers in diameter and a few micrometers in length is an exciting challenge, which led only a few years after the discovery of CNTs to the first studies concerning their opening, filling, capillarity, and wetting.[1] The complete filling of CNTs, which allows for the production of metallic nanowires[2] for electronic or magnetic devices, has been mastered and well-documented.[3] However, the selective confinement of discrete nanoparticles (NPs) in the CNT cavity is still a synthetic challenge. Success in this endeavor could pave the way to interesting perspectives for drug delivery or for performing chemistry in a confined space while exploiting the unique CNT properties. Owing to synthetic difficulties, few studies provide results on confinement effects in CNTs. For example, the reactivity of iron oxide NPs is increased (easy reduction), while that of metallic iron NPs is decreased (difficult reoxidation) when confined inside CNTs.[4] Dimensionally confined phase transitions have been reported for water[5] and ionic liquids[6] encapsulated within CNTs. Heptene confined in CNTs shows a reduced reactivity towards atomic hydrogen,[7] and rhodium NPs confined in CNTs are one order of magnitude more active for ethanol production from syngas than their counterparts deposited on the convex CNT surface.[8] Furthermore, the ultraefficient transport of water and gas through the hydrophobic cavity of CNTs makes CNT membranes promising for many applications.[9]

Currently, three main routes are used to introduce NPs inside CNTs: 1) Incipient wetness impregnation techniques rely on the filling of oxidized CNTs by capillarity with a solution containing a metal salt[10–15] or preformed NPs.[16] X-ray photoelectron spectroscopy (XPS)[11] and 3D TEM[12] studies have indicated that the fraction of metal present in the inner cavity of CNTs is between 15 and 50%. More selective filling of very large diameter (300 nm or larger) carbon filaments by preformed NPs has been achieved. 2) Sublimation of a metal precursor can be used to introduce it into the CNT cavity.[17] For these two methods, an improvement in the confinement selectivity can be obtained if an additional selective washing step is performed to eliminate NPs deposited on the external surface.[18] The main drawback of these methods is that a significant amount of precursor is lost during the synthesis. 3) Another multistep approach consists of producing CNTs inside anodic aluminum oxide membranes, filling the resulting template with a solution of NPs, and dissolving the alumina membrane.[19] This latter method, however, suffers from scale-up difficulties.

Herein we report 1) a simple and efficient method for the selective confinement of NPs in the inner cavity of CNTs, and 2) the effect of spatial confinement of bimetallic PtRu NPs on their catalytic performance for the selective hydrogenation of cinnamaldehyde. The strategy we have developed to selectively confine NPs inside CNTs is based on surface chemistry (Figure 1).

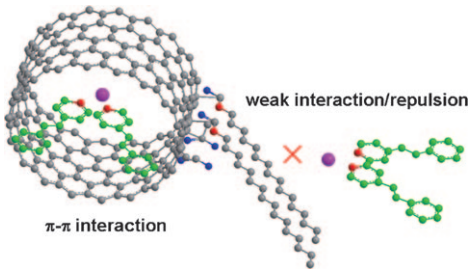

Figure 1. Strategy adopted to drive NPs into CNTs. PtRu NPs pink, N red, O blue, C gray and green.

[*] Dr. E. Castillejos, Dr. A. Solhy, Dr. P. Serp
CNRS; LCC (Laboratoire de Chimie de Coordination)
composante ENSIACET
118, route de Narbonne, 31077 Toulouse (France)
and
Université de Toulouse; UPS, INP; LCC
31077 Toulouse (France)
Fax: (+33) 5-6288-5600
E-mail: philippe.serp@ensiacet.fr
Homepage: http://www.lcc-toulouse.fr/

Dr. P.-J. Debouttière, Dr. V. Martinez, Dr. K. Philippot, Dr. B. Chaudret
CNRS; LCC (Laboratoire de Chimie de Coordination)
205, route de Narbonne, 31077 Toulouse (France)
and
Université de Toulouse; UPS, INP; LCC
31077 Toulouse (France)

Dr. Y. Kihn
CEMES, CNRS UPR 8001
29 Rue Jeanne Marvig, 31055 Toulouse (France)

L. Roiban, Dr. O. Ersen
IPCMS—Groupe Surfaces et Interfaces, CNRS—ULP UMR 7504
23 Rue du Loess BP 43, 67034 Strasbourg (France)

[**] This work was performed under ANR PNano 2005 ANR-05-NANO-030-01. Vincent Collière is acknowledged for technical assistance in TEM imaging, and Dr. D. Gonbeau (CNRS, Pau, France) for her help in the XPS experiments.

Supporting information for this article is available on the WWW under http://dx.doi.org/10.1002/anie.200805273.

The first step consists of the controlled preparation by an organometallic route[20] of NPs stabilized by a ligand possessing two functionalities: one has an affinity for the surface of the NPs and the other presents an affinity for the CNT graphene layers (π–π interaction). We have chosen 4-(3-phenylpropyl)pyridine (L) as ligand, as it may coordinate to NPs by the nitrogen atom of the pyridine group and may interact with the CNT surface through the phenyl ring. The second step is the functionalization of CNT external surface to introduce different surface species that should induce weak interaction or repulsion between the NPs and CNT external surface. Thus, we have introduced two kinds of functionalities on CNT surface, carboxylic acid groups and amide groups presenting a long alkyl chain.

The pristine CNTs, denoted CNT1, present a specific surface area of $38\,m^2g^{-1}$, a mesoporous volume of $0.15\,cm^3g^{-1}$, a mean pore diameter of 16 nm (inner hollow cavities and aggregated pores formed by interaction of isolated CNTs), an average external diameter of 80 nm, and an average internal diameter of 40 nm, and they do not present graphene layers perpendicular to the CNT axis. To facilitate the introduction of NPs into the CNT cavity, the CNTs were segmented (0.1–1 μm) by ball-milling to open both their ends (see the Supporting Information). The functionalization of the segmented CNT1 surface with carboxylic acid groups was achieved by nitric acid oxidation,[21] yielding CNT2. To graft moieties terminated by long alkyl chains onto the CNT surface, CNT2 was treated with thionyl chloride to produce acetyl chloride groups and further treated with hexadecylamine (HDA) to produce the amide surface groups of CNT3 (Figure 2). CNT1–3 have been characterized by TEM, IR spectroscopy, thermogravimetric analysis, elemental analysis, chemical titration, and XPS.

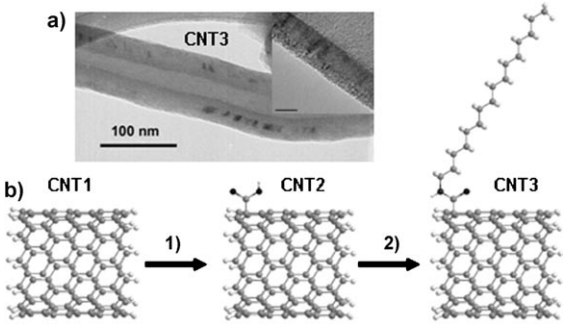

Figure 2. a) TEM micrograph of CNT3; the inset shows an enlargement of the CNT wall, scale bar 10 nm. b) CNT functionalization: 1) HNO_3 oxidation at 413 K for 3 h; 2) $SOCl_2$ and HDA.

As-received CNT1 nanotubes are open and present a low amount of surface oxygen functionalities (Table 1). Nitric acid treatment allows the introduction of polar hydrophilic surface groups, mainly carboxylic acid groups but also phenol, carbonyl, and quinone functionalities.[22] The duration of this treatment was limited to 3 h to avoid internal surface functionalization; this treatment also induces a burn-off of approximately 3%, as evidenced by the results of elemental analysis (Table 1). The concentration of surface carboxylic acid groups in CNT2 is 1 $mmol\,g^{-1}$, as determined by chemical titration (see the Supporting Information).[23] The reaction of surface carboxyl and phenol groups of CNT-2 with thionyl chloride leads to acetyl moieties.[24] Hexadecylamine reacts with the acetyl groups to produce the amide species, but it can also react with carbonyl groups to produce the imine functionality.[25] The effective grafting of the long alkyl chain onto the CNT3 surface has been verified by IR spectroscopy. Besides the bands at 1580 cm^{-1} from CNT skeletal in-plane vibration and at 1721 cm^{-1} attributed to the ν_{asym}(COOH) of carboxylic acid groups (from hydrolysis of some acetyl chloride groups[24]), the spectra of CNT3 show a band at 1635 cm^{-1} consistent with the amide functionality and the aliphatic C–H stretching bands located between 2850 and 2950 cm^{-1} (see the Supporting Information). The bulk quantitative (elemental analysis) and surface semiquantitative (XPS) analyses confirm the functionalization of CNTs (Table 1). Furthermore, thermogravimetric analyses under air and under nitrogen show that around 50% of the carboxylic acid groups have reacted with HDA (see the Supporting Information).

Table 1: Elemental and XPS analyses of as-received and functionalized CNTs.

	XPS [atom%]			Elemental analysis [wt%]		
	C	O	N	C	O	N
CNT1	98.6	1.4	–	96.3	0.4	0.6
CNT2	86.1	13.9	–	83.2	8	0.5
CNT3	90.2	9.8	–	88.8	3.3	1.1

Platinum–ruthenium nanoparticles were prepared at room temperature through the co-decomposition of [Ru(η^4-1,5-cod)(η^6-1,3,5-cot)] (cod = cyclooctadiene; cot = cyclooctatriene) and [Pt(CH_3)$_2$(η^4-1,5-cod)] in the presence of L under dihydrogen, using a procedure similar to previously reported ones (see the Supporting Information).[20] Under these conditions, small and homogeneously dispersed nanoparticles showing a quite narrow size distribution around a mean diameter of 2.2 ± 0.7 nm were obtained (Figure 3). The weight elemental composition of these NPs is Pt 40%, Ru 18%, and L 42%. Even if we do not yet know if they are alloyed or core–shell NPs, X-ray microanalysis confirms the

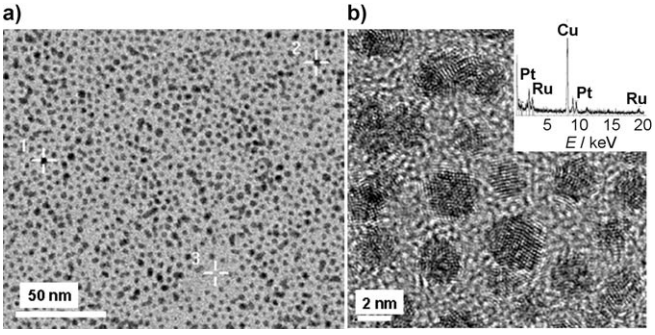

Figure 3. a) TEM and b) HREM images of PtRu NPs. The inset in (b) shows the energy-dispersive X-ray spectrum. The points marked 1, 2, and 3 in (a) highlight the particles selected for EDX spectra.

bimetallic nature of these nanoparticles (Figure 3). Although we have not yet studied the coordination of L on PtRu NPs, a recent report has shown that L can coordinate on Ru NPs.[26]

Two synthetic routes have been followed for the preparation of 5–23 wt% PtRu–CNT samples. The first one consists of a simple impregnation procedure performed on CNT1–3 in THF, an organic solvent presenting a low surface tension (26 mN m^{-1}), which should wet and penetrate inside CNTs. The samples prepared in this way were named PtRu@CNT1–3. The second one consists of the co-decomposition of the Pt and Ru precursors in the presence of L and CNT2 (PtRu/CNT2). It was performed to favor the nucleation of NPs on the outer surface of CNTs; indeed, the presence of surface COOH anchoring sites should enhance the nucleation of PtRu NPs. TEM (Figure 4) and 3D TEM[12] (Figure 5) have been used to determine the spatial location of PtRu NPs in the different samples. For PtRu@CNT1, where π–π interactions may occur on both the concave and convex surfaces, the confinement of PtRu NPs is clearly not selective (Figures 4a and 5b), and most of the NPs are visible on the external surface. On this support, PtRu NPs are nicely dispersed at 5 wt% loading (not shown) and started to agglomerate in aggregates of a few NPs at 11 wt% loading. 3D TEM performed on 11% PtRu@CNT1 confirms that the NPs are located on both the inside and outside of CNT1 (Figure 5b). Although a precise quantification is difficult to establish, by analyzing the 3D TEM reconstructed volume of the chosen CNT we have estimated that approximately 30% of the PtRu NPs are located inside the CNT1 cavity. Interestingly, the mean diameter of NPs located inside CNT1 (1.6 nm) is smaller than that of NPs deposited on CNT1 (2 nm; see the Supporting Information). For PtRu@CNT2, the NPs show a tendency to agglomerate in large aggregates of NPs on the outer surface of CNTs, regardless of metal loading (Figure 4b). For these samples, fewer NPs are confined in the interior of CNTs than for CNT1. For PtRu@CNT3, a remarkable effect of CNT functionalization on NP location was observed, since most of the NPs are located inside CNTs, regardless of metal loading (5–23 wt%; see the Supporting Information). For the 23% sample (Figure 4c), 3D TEM measurements show that 80% of PtRu/L NPs are confined in the inner cavity of the CNTs (Figure 5c), which is a significant improvement compared to classical techniques. There also, NPs located inside CNTs (2 nm) present a lower mean diameter than the NPs deposited on CNT external surface (2.5 nm; see the Supporting Information). The steric hindrance arising from the long alkyl chain, in combination with the weak interaction that should occur between the alkyl groups of the CNT3 surface and PtRu/L NPs (Figure 1), seems a reasonable explanation of these results. Between 5 and 11 wt% NPs, most of the PtRu NPs are located on the internal graphene layers, and at higher loadings the CNT inner cavity is really stuffed with NPs. At the highest loading (23 wt%), π–π interactions between the ligands of different particles should prevail to stabilize the NPs. Finally, for PtRu/CNT2 (Figure 4d), 3D TEM shows that around 90% of the nanoparticles are located on the external CNT surface (Figure 5a). For that sample, for which preformed NPs have not been used, the mean NP size is 2.2 nm, regardless of NP location (see the Supporting Information).

To get more macroscopic information on NP location, we also performed XPS analyses on PtRu@CNT1, PtRu/CNT2, and PtRu@CNT3 at various metal loadings (Figure 6). The

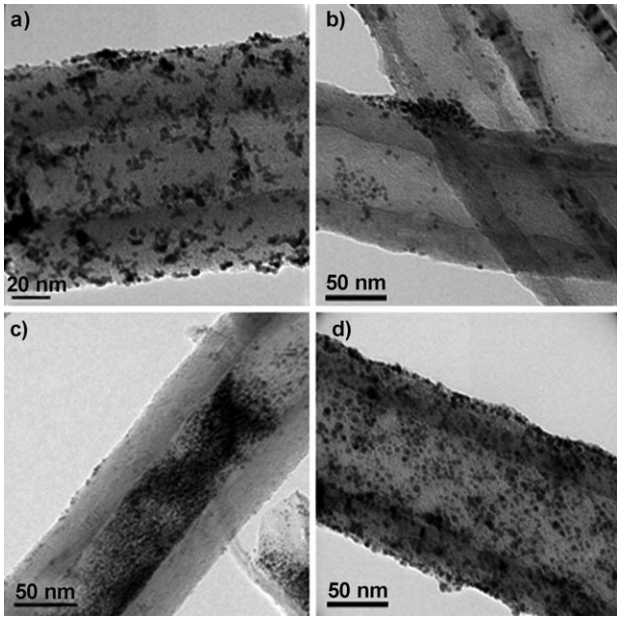

Figure 4. 2D TEM images of a) 11 wt% PtRu@CNT1, b) 5 wt% PtRu@CNT2, c) 23 wt% PtRu@CNT3, and d) 5 wt% PtRu/CNT2.

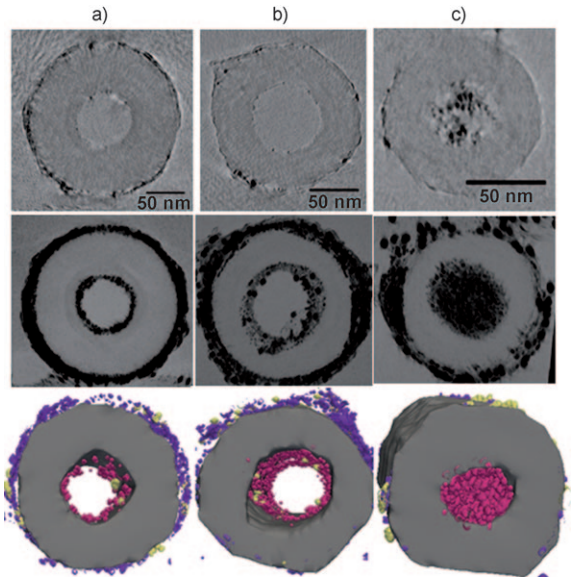

Figure 5. Top: examples of transverse sections extracted from the reconstruction, middle: minimum-intensity projections of all sections on the same plane to highlight the contribution of the NPs, and bottom: modeling of the reconstruction of a) 5 wt% PtRu/CNT2, b) 11 wt% PtRu@CNT1, and c) 23 wt% PtRu@CNT3. The large, round-shape NPs on transverse sections and global projections are Au NPs deposited before 3D TEM analysis to facilitate the treatment of the tilt series for the reconstruction (see the Supporting Information): violet PtRu NPs outside, red PtRu NPs inside, and yellow Au NPs.

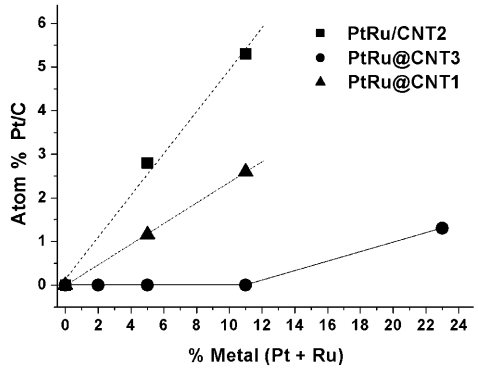

Figure 6. External surface Pt content (atom %) in PtRu@CNT1, PtRu/CNT2, and PtRu@CNT3 for different metal loadings (as determined by XPS).

XPS data confirm the results obtained at the local scale by 3D TEM. Moreover, it seems that below 11 wt % metal, the percentage of NPs located inside CNT3 is close to 100 %. To our knowledge, such a control of NP location in the inner cavity or on the external surface of open-ended CNTs is unprecedented.

To evaluate the effect of confinement of NPs on their catalytic performance, we compared four catalytic systems (PtRu@CNT1, PtRu@CNT3, PtRu/CNT2, and PtRu/L NPs) for the reaction of selective hydrogenation of cinnamaldehyde (CAL). The targeted but thermodynamically unfavored reaction is the hydrogenation of the carbonyl group to produce the cinnamyl alcohol (COL). Alternative routes involve the reduction of the olefinic C=C bond, leading to hydrocinnamaldehyde (HCAL), and the complete hydrogenation to produce the fully saturated hydrocinnamyl alcohol (HCOL). Platinum,[27–29] platinum-based,[30,31] and palladium[10] catalysts on CNTs have already been investigated for this reaction, and bimetallic systems[30,31] generally permit higher selectivity towards COL than monometallic ones.

Control experiments performed at 20 bar H_2 and 343 K show that CNTs do not present any activity for this reaction. In the presence of the catalysts, and under the reaction conditions employed, the sole products of CAL hydrogenation were COL, HCAL, and HCOL. Considering that the tests were performed with NPs of the same size and with CNTs of the same diameter, we noticed a remarkable effect of NP location on both activity and selectivity (Table 2). First, the presence of CNTs as a support allows an increase of both activity and selectivity, since unsupported PtRu/L NPs are significantly less active and selective. Furthermore, when NPs are located mainly inside (PtRu@CNT3) and not outside (PtRu/CNT2) CNTs, a very high selectivity towards COL formation was observed. In fact, evidence for a linear relationship between selectivity and the percentage of NPs located inside CNTs have been established (see the Supporting Information).

Increasing the loading of NPs on CNT3 from 5 to 23 % induces a further increase in selectivity towards COL to 100 % and a decrease of the TOF to 41 h^{-1}. Besides the high concentration of NPs inside CNT3, a reasonable explanation

Table 2: Catalytic results for cinnamaldehyde hydrogenation.[a]

Catalyst	NPs d_{mean} [nm]	% NP int.	TOF [h^{-1}]	HCAL	HCOL	COL
PtRu/L NPs	2.2	–	30	50	15	35
PtRu/CNT2	2.2/2.2[b]	10	56	33	8	59
PtRu@CNT1	1.6/2.2[b]	30	75	18	12	69
PtRu@CNT3	2/2.5[b]	80	85	0	5	95

[a] See the Supporting Information for experimental conditions. [b] d_{mean} of NPs inside/d_{mean} of NPs outside.

of the remarkable performance of this system could be the adsorption properties of CNTs, which, particularly for CNT3 where the external surface is passivated by the long-chain amide, should permit an increase in the concentration of CAL around the active NPs present in the internal cavity. Indeed, it has been shown that the activity of Pt catalysts increases with the initial CAL concentration.[32]

Furthermore, it has been proposed that at high CAL concentration the CAL molecules adsorb perpendicular to the Pt surface with the aromatic ring in a parallel arrangement, thereby enhancing the selectivity towards COL.[32] Finally, a higher concentration of active hydride species was reported when Rh NPs were located inside rather than outside CNTs.[8] Thus, the confinement of CAL and NPs into CNT3, for which the outside surface is functionalized with the long alkyl chain, is expected to give the highest activity and selectivity.

In conclusion, we report a simple and selective procedure, based on molecular recognition, to build a nanoreactor consisting of approximately 2 nm PtRu nanoparticles confined in segmented CNTs of 40 nm internal diameter. These nanocatalysts display excellent catalytic performance owing to confinement of both the active phase and the reactants in the inner cavity of CNTs.

Received: October 28, 2008
Published online: February 26, 2009

Keywords: carbon nanotubes · confinement · heterogeneous catalysis · hydrogenation · nanoparticles

[1] a) P. M. Ajayan, S. Iijima, *Nature* **1993**, *361*, 333–334; b) S. C. Tsang, Y. K. Chen, P. J. F. Harris, M. L. H. Green, *Nature* **1994**, *372*, 159–162; c) E. Dujardin, T. W. Ebbesen, H. Hiura, K. Tanigaki, *Science* **1994**, *265*, 1850–1852.
[2] a) C. Pham-Huu, N. Keller, C. Estournès, G. Ehret, M. J. Ledoux, *Chem. Commun.* **2002**, 1882–1883; b) J. Hu, Y. Bando, J. Zhan, C. Zhi, D. Golberg, *Nano Lett.* **2006**, *6*, 1136–1140.
[3] M. Monthioux, *Carbon* **2002**, *40*, 1809–1823.
[4] W. Chen, X. Pan, X. Bao, *J. Am. Chem. Soc.* **2007**, *129*, 7421–7426.
[5] K. Koga, G. T. Gao, H. Tanaka, X. C. Zeng, *Nature* **2001**, *412*, 802–805.
[6] S. Chen, G. Wu, M. Sha, S. Huang, *J. Am. Chem. Soc.* **2007**, *129*, 2416–2417.
[7] P. Kondratyuk, J. T. Yates, Jr., *J. Am. Chem. Soc.* **2007**, *129*, 8736–8739.

[8] X. Pan, Z. Fan, W. Chen, Y. Ding, H. Luo, X. Bao, *Nat. Mater.* **2007**, *6*, 507 – 511.
[9] A. Noy, H. G. Park, F. Fornasiero, J. K. Holt, C. P. Grigoropoulos, O. Bakajin, *Nano Today* **2007**, *2*, 22 – 29.
[10] J.-P. Tessonnier, L. Pesant, G. Ehret, M. J. Ledoux, C. Pham-Huu, *Appl. Catal. A* **2005**, *288*, 203 – 210.
[11] F. Winter, G. Leendert Bezemer, C. vand der Spek, J. D. Meeldijk, A. J. van Dillen, J. W. Geus, K. P. de Jong, *Carbon* **2005**, *43*, 327 – 332.
[12] O. Ersen, J. Werckmann, M. Houllé, M. J. Ledoux, C. Pham-Huu, *Nano Lett.* **2007**, *7*, 1898 – 1907.
[13] H.-Q. Wu, X.-W. Wei, M.-W. Shao, J.-S. Gu, M.-Z. Qu, *J. Mater. Chem.* **2002**, *12*, 1919 – 1921.
[14] A. M. Zhang, J. L. Dong, Q. H. Xu, H. K. Rhee, X. L. Li, *Catal. Today* **2004**, *93–95*, 347 – 352.
[15] J. Zhang, Y.-S. Hu, J.-P. Tessonnier, G. Weinberg, J. Maier, R. Schlögl, D. S. Su, *Adv. Mater.* **2008**, *20*, 1450 – 1455.
[16] a) B. M. Kim, S. Qian, H. H. Bau, *Nano Lett.* **2005**, *5*, 873 – 878; b) A. V. Bazilevsky, K. Sun, A. L. Yarin, C. M. Megaridis, *J. Mater. Chem.* **2008**, *18*, 696 – 702.
[17] a) P. M. F. J. Costa, J. Sloan, T. Rutherford, M. L. H. Green, *Chem. Mater.* **2005**, *17*, 6579 – 6582; K. Schulte, J. C. Swarbrick, N. A. Smith, F. Bondino, E. Magnano, A. N. Khlobystov, *Adv. Mater.* **2007**, *19*, 3312 – 3316.
[18] a) D. Jain, R. Wilhelm, *Carbon* **2007**, *45*, 602 – 606; b) A. Capobianchi, S. Foglia, P. Imperatori, A. Notargiacomo, M. Giamatteo, T. Del Buono, E. Palange, *Carbon* **2007**, *45*, 2205 – 2208; c) Q. Fu, G. Weinberg, D.-S. Su, *New Carbon Mater.* **2008**, *23*, 17 – 20.
[19] a) G. Korneva, H. Ye, Y. Gogotsi, D. Halverson, G. Friedman, J.-C. Bradley, K. G. Kornev, *Nano Lett.* **2005**, *5*, 879 – 884; b) X.-H. Wang, H. Orikasa, N. Inokuma, Q.-H. Yang, P.-X. Hou, H. Oshima, K. Iyoh, T. Kyotani, *J. Mater. Chem.* **2007**, *17*, 986 – 991; c) H. Orikasa, N. Inokuma, S. Ittisanronnachai, X. H. Wang, O. Kitakami, T. Kyotani, *Chem. Commun.* **2008**, 2215 – 2217.
[20] a) B. Chaudret, *C. R. Phys.* **2005**, *6*, 117 – 131; b) K. Philippot, B. Chaudret in *Comprehensive Organometallic Chemistry III*, *Vol. 12* (Ed.: R. H. Crabtree, M. P. Mingos, D. O'Hare), Elsevier, Amsterdam, **2007**, chap. 12-03, p. 71.
[21] A. Solhy, B. F. Machado, J. Beausoleil, Y. Kihn, F. Gonçalves, M. F. R. Pereira, J. J. M. Órfão, J. L. Figueiredo, J. L. Faria, P. Serp, *Carbon* **2008**, *46*, 1194 – 1207.
[22] T. I. T. Okpalugo, P. Papakonstantino, H. Murphy, J. McLaughlin, N. M. D. Brown, *Carbon* **2005**, *43*, 153 – 161.
[23] M. L. Toebes, J. M. P. van Heeswijk, J. H. Bitter, A. Jos van Dillen, K. P. de Jong, *Carbon* **2004**, *42*, 307 – 315.
[24] M. Breza, *Chem. Phys.* **2006**, *330*, 224 – 230.
[25] A. R. Silva, M. Martins, M. M. A. Freitas, J. L. Figueiredo, C. Freire, B. De Castro, *Eur. J. Inorg. Chem.* **2004**, 2027 – 2035.
[26] I. Favier, S. Massou, E. Teuma, K. Philippot, B. Chaudret, M. Gómez, *Chem. Commun.* **2008**, 3296 – 3298.
[27] H. Ma, L. Wang, L. Chen, C. Dong, W. Yu, T. Huang, Y. Qian, *Catal. Commun.* **2007**, *8*, 452 – 456.
[28] X. Lepró, E. Terrés, Y. Vega-Cantú, F. J. Rodríguez-Macías, H. Muramatsu, Y. A. Kim, T. Hayahsi, M. Endo, M. Torres R. , M. Terrones, *Chem. Phys. Lett.* **2008**, *463*, 124 – 129.
[29] Z. T. Liu, C.-X. Wang, Z.-W. Liu, J. Liu, *Appl. Catal. A* **2008**, *344*, 114 – 123.
[30] H. Vu, F. Gonçalves, R. Philippe, E. Lamouroux, M. Corrias, Y. Kihn, D. Plee, P. Kalck, P. Serp, *J. Catal.* **2006**, *240*, 18 – 22.
[31] Y. Li, Z.-G. Li, R.-X. Zhou, *J. Mol. Catal. A* **2008**, *279*, 140 – 146.
[32] M. L. Toebes, T. A. Nijhuis, J. Hájek, J. H. Bitter, A. J. van Dillen, D. Y. Murzin, K. P. de Jong, *Chem. Eng. Sci.* **2005**, *60*, 5682 – 5695.

